SAND2014-15572PE

Exceptional service in the national interest

Sandia National Laboratories

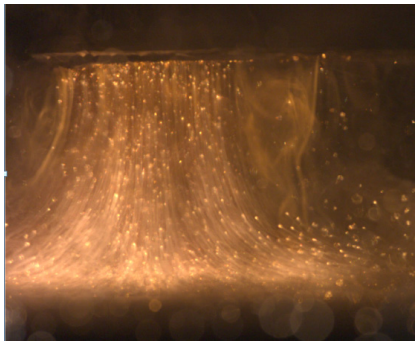

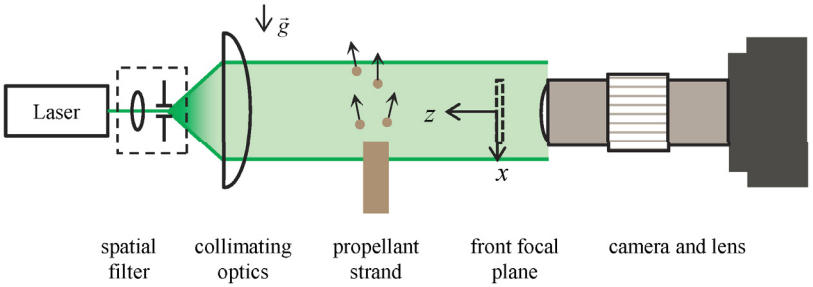

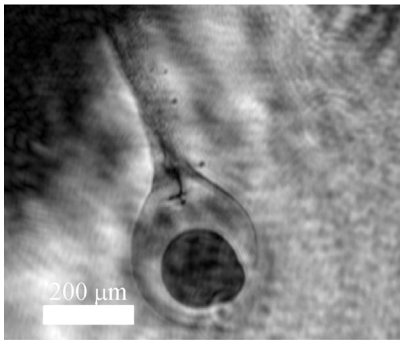

Digital In-Line Holography (DIH) for 3D Imaging of Aluminum Drop Combustion in Propellant Plumes

Daniel R. Guildenbecher

July 14, 2014

U.S. DEPARTMENT OF ENERGY | NNSA National Nuclear Security Administration

Sandia National Laboratories is a multi-program laboratory managed and operated by Sandia Corporation, a wholly owned subsidiary of Lockheed Martin Corporation, for the U.S. Department of Energy's National Nuclear Security Administration under contract DE-AC04-94AL85000.

Motivation: 3D imaging for a 3D world

Widely available 2D imaging or point-wise measurement techniques are often insufficient to resolve 3D flow phenomena

- Repetition needed to capture spatial statistics

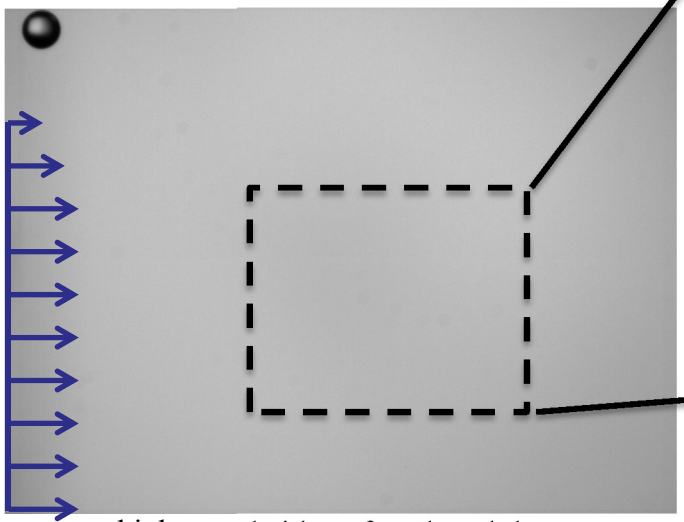

high-speed video of a ethanol drop in an air-stream

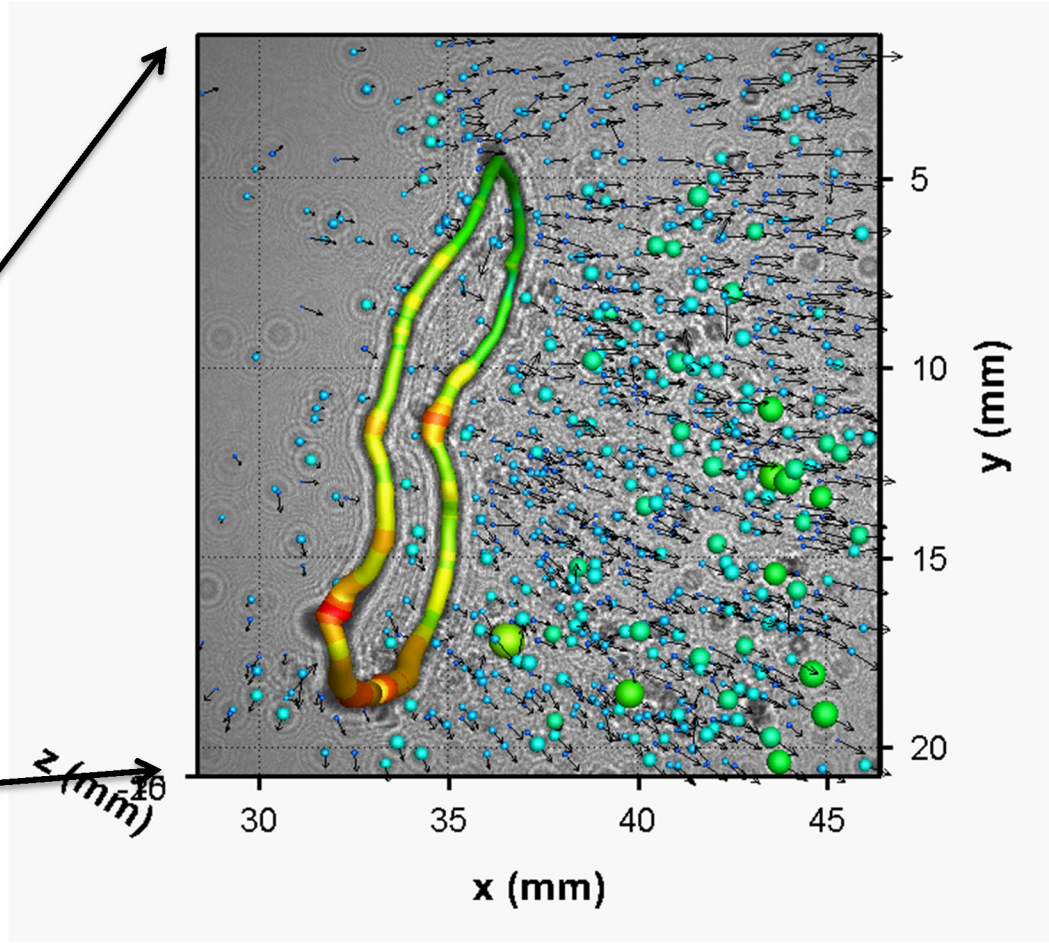

digital holographic measurement (Gao et al, 2013, *Opt. Lett.*)

Holography is an optical technique to record and reconstruct a 3D light field

What is holography?

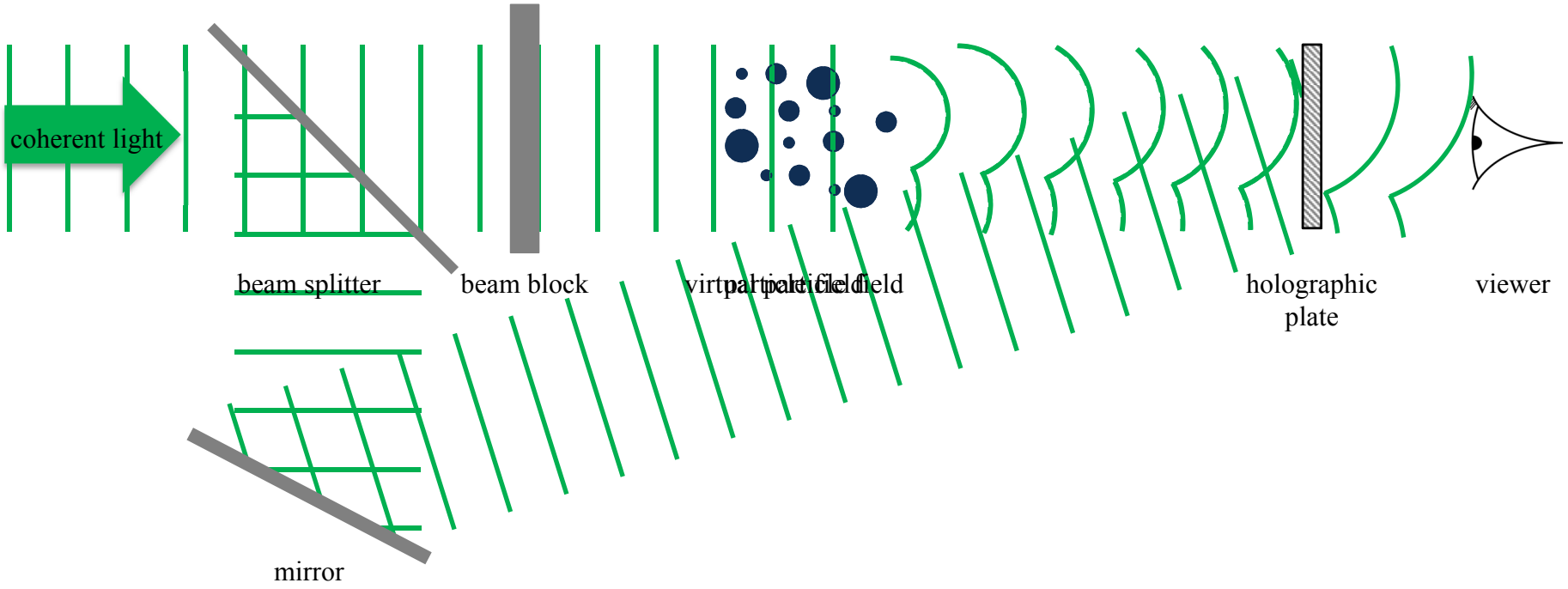

Optical method first proposed by Gabor in 1948

1. Coherent light scattered by particle field forms the object wave, E_o
2. Interference with a reference wave, E_r, forms the hologram: $h = |E_o+E_r|^2$
3. Reconstruction with E_r forms virtual images at original particle locations

$$h \cdot E_r = \underbrace{(|E_o|^2 + |E_r|^2)E_r}_{\text{DC term}} + \underbrace{|E_r|^2 E_o}_{\text{virtual image}} + \underbrace{E_r^2 E_o^*}_{\text{real image}}$$

Digital in-line holography (DIH)

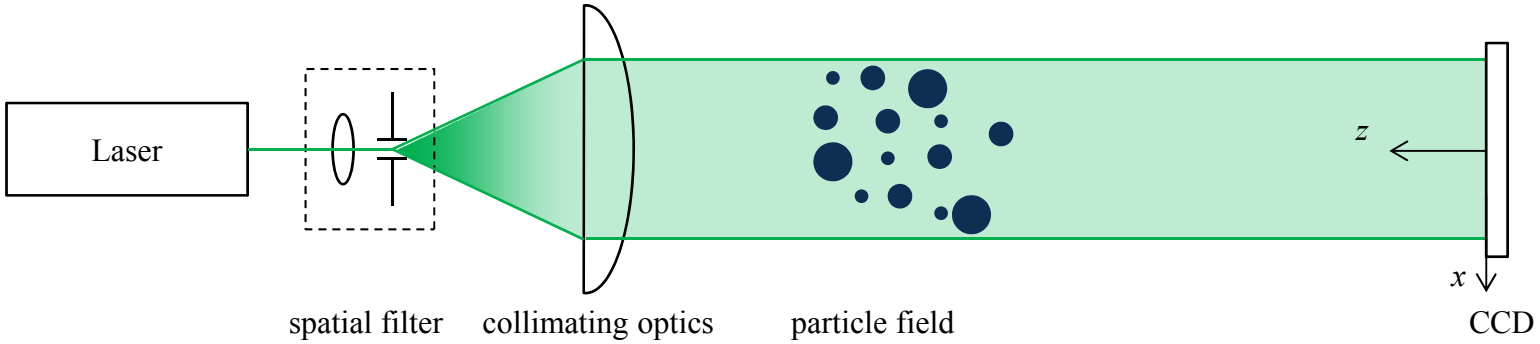

Holographic plate and wet-chemical processing replaced with digital sensor

- First proposed by Schnars and Jüptner in '90s
- Advantage: hologram can be numerically refocused using the diffraction integral equation
- Challenge: Resolution of digital sensors (order 100 line pairs/mm) is much less than resolution of photographic emulsions (order 5,000 line pairs/mm)
  - For suitable off axis angles, θ, the fringe frequency, f, is typically too large to resolve with digital sensors ($f = 2\sin(\theta/2)/\lambda$)
  - Rather, the in-line configuration ($\theta = 0$) is typically utilized

Digital in-line holography (DIH)

- In the computer, we multiply the digitally recorded hologram *h* by an estimate of the complex conjugate of the reference wave E_r^*

$$h \cdot E_r^* = \underbrace{(|E_o|^2 + |E_r|^2)E_r^*}_{\text{DC term}} + \underbrace{E_r^{*2}E_o}_{\text{virtual image}} + \underbrace{|E_r|^2 E_o^*}_{\text{real image}}$$

- This complex amplitude can be numerically propagated to any distance along the optical axis, z, using the diffraction equations

$$E(x,y,z) = h(x,y) \cdot E_r^*(x,y) \otimes g(x,y,z)$$

  - Rayleigh-Sommerfeld: $g(x,y,z) = e^{jk\sqrt{x^2+y^2+z^2}} \Big/ j\lambda\sqrt{x^2+y^2+z^2}$
  - Fresnel-Kirchhoff: $g(x,y,z) = \frac{e^{jkz}}{j\lambda z} e^{jk\left(x^2+y^2\right)/2z}$

- Numerically, the convolution is computed using the fast Fourier transform (FFT)

$$E(x,y,z) = FFT^{-1}\left\{FFT\left\{I_0(x,y)E_r^*(x,y)\right\}FFT\left\{g(x,y,z)\right\}\right\}$$

- Visualized via the reconstructed amplitude, $A = |E|$, or intensity, $I = |E|^2$

Digital in-line holography (DIH)

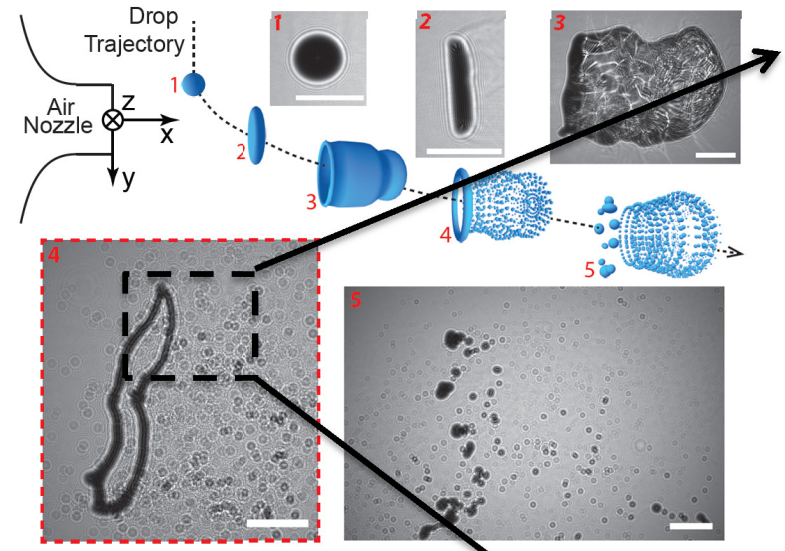

digital holograms of the breakup of an ethanol drop in an air-stream (Gao et al 2013, *Opt. Lett.*)

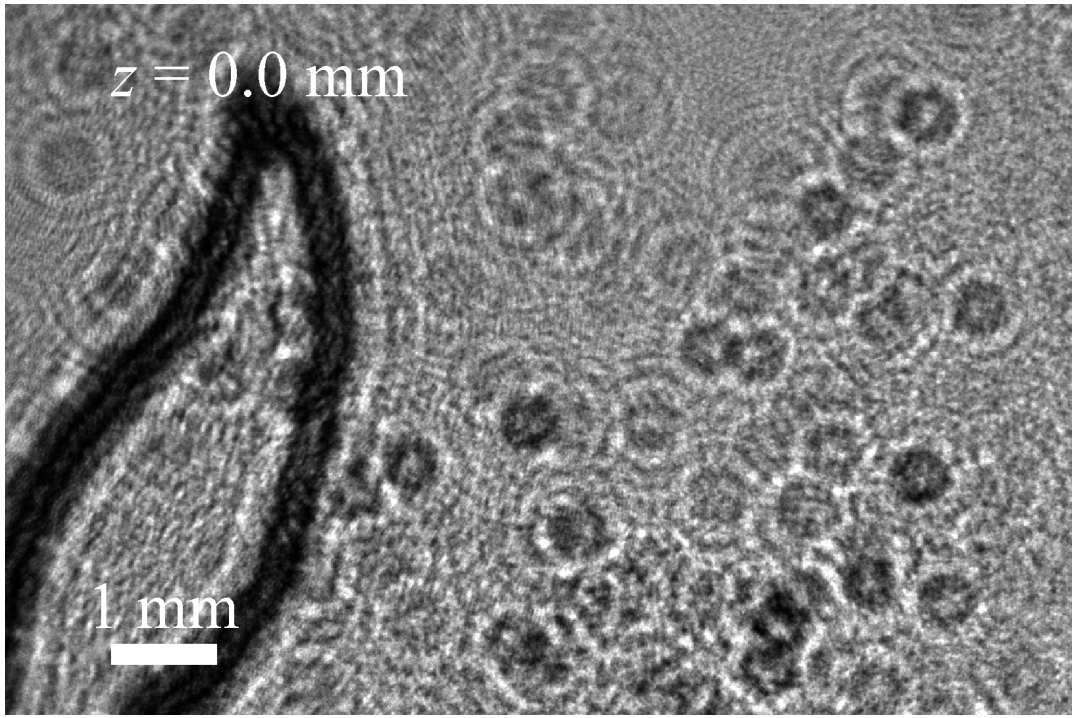

Reconstructed amplitude throughout depth, *z*

- In-focus structures are clearly observed at different depths, *z*
- "Rings" around the in-focus structures are the out-of-focus virtual images

How can we automatically extract in-focus objects and validate the accuracy of the results?

Hybrid particle extraction method

Sandia National Laboratories

Basic idea: In-focus regions display a minimum amplitude within the particle interior and a maximum sharpness at the particle edges

- Validity of this assumption has been verified through simulation

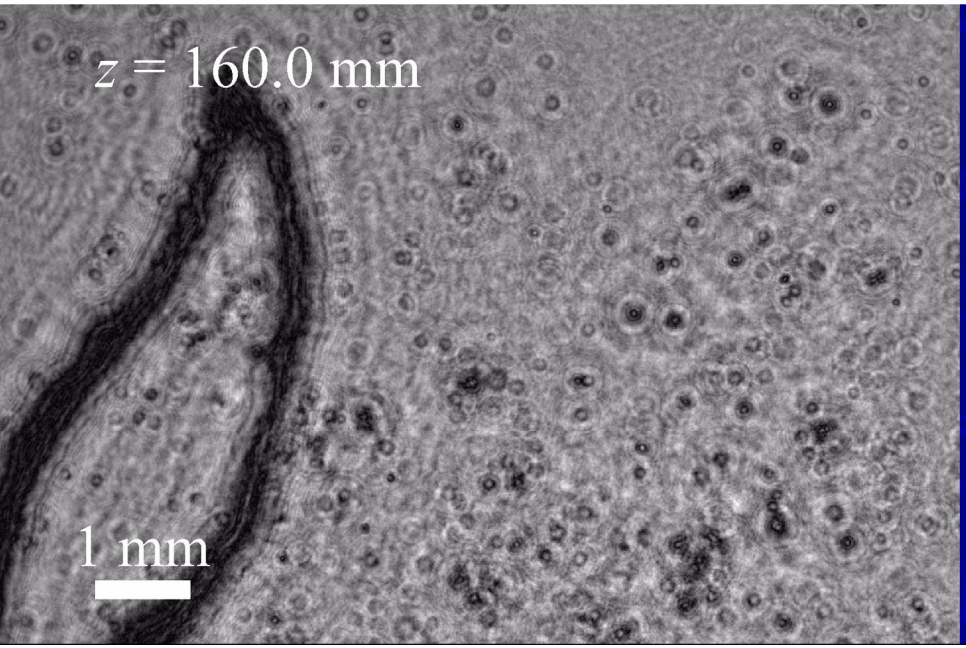

Reconstructed amplitude throughout depth, z

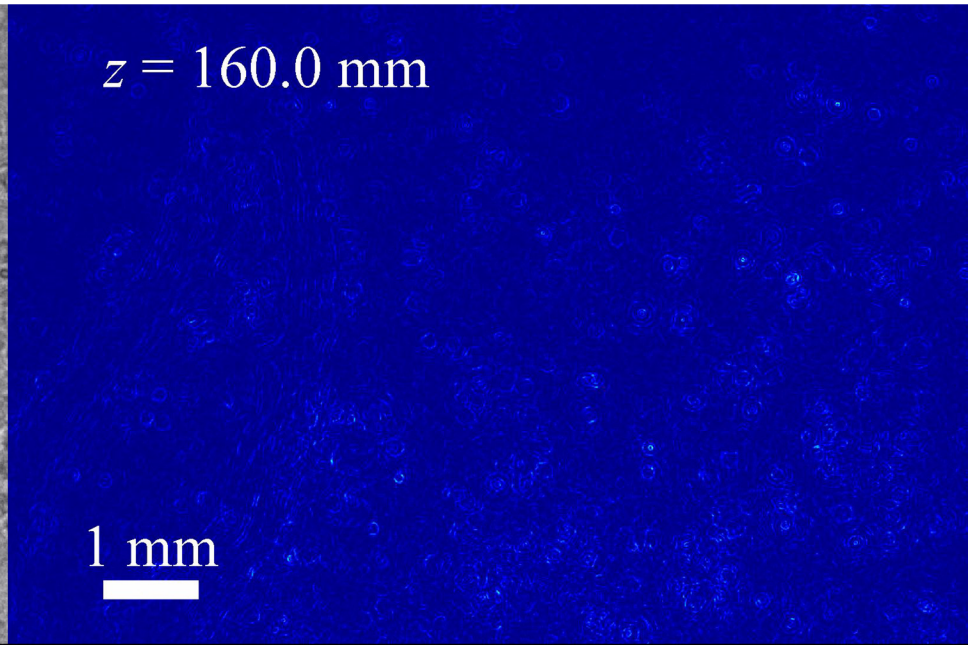

Reconstructed edge sharpness throughout depth, z

- Optimum segmentation threshold is automatically extracted from the threshold of the amplitude which displays maximum edge sharpness
  - Further details in Guildenbecher et al, 2013, *Appl. Opt.* and Gao et al, 2013, *Opt. Express.*

Experimental validation

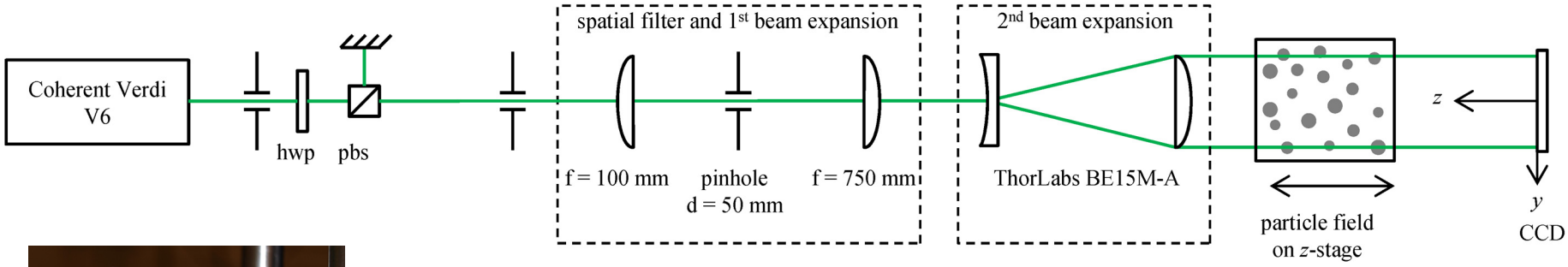

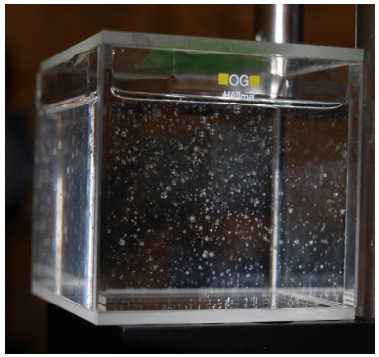

particle field

- Quasi-stationary particle field
  - Polystyrene beads ($\bar{d} \approx 465\,\mu m$) in 10,000 cSt silicone oil
  - Settling velocity ≈ 0.8 µm/s
- Multiple holograms recorded, displacing the particle field 2 mm in the *z*-direction between each acquisition

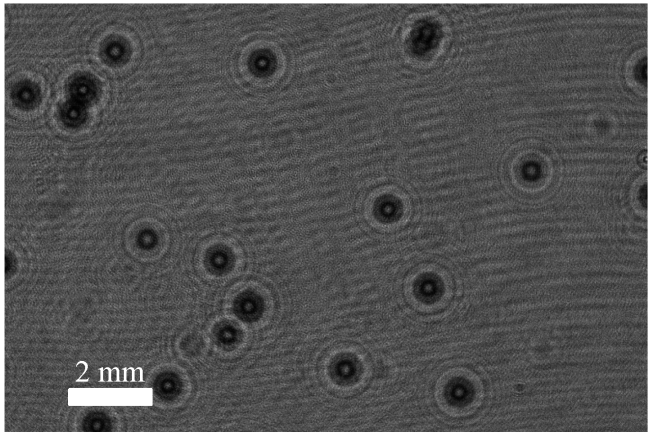

hologram

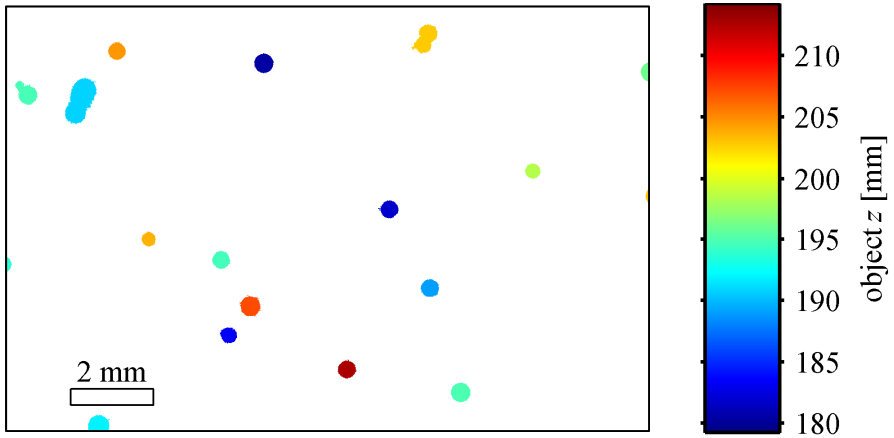

Detected objects colored by *z*-position

Experimental validation

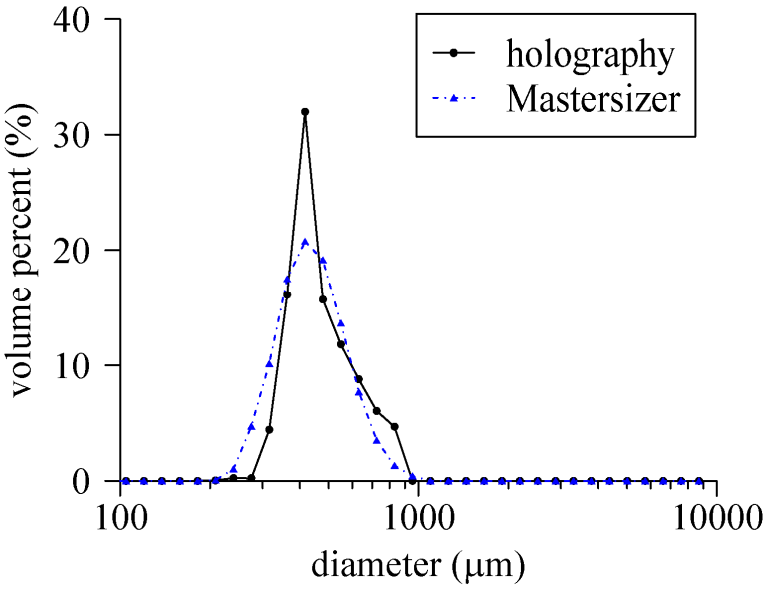

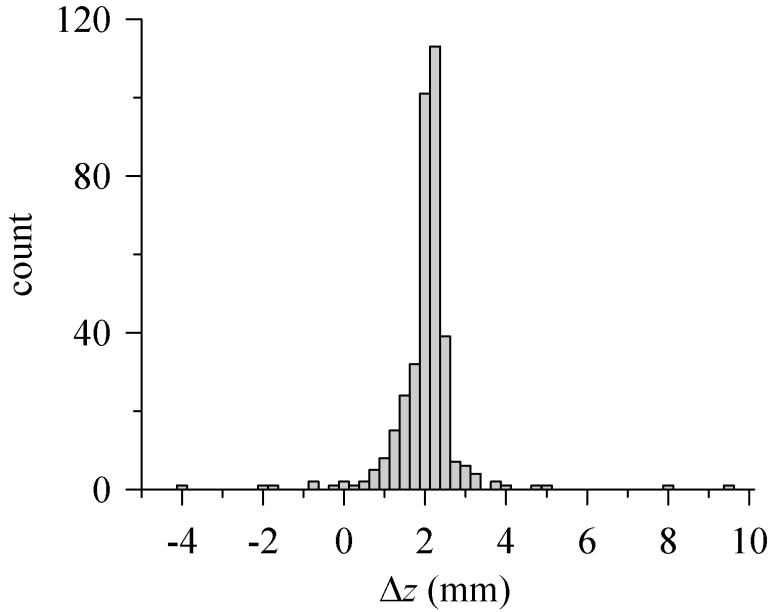

Diameter measured from area of the detected 2D morphology

- Actual mass median diameter = 465 μm
- Measured mass median diameter = 474 μm
  - Error of 2.0% with respect to actual value

Displacement found by particle matching between successive holograms

- Actual displacement = 2.0 mm
- Mean detected displacement = 1.91 mm +/- 0.81 mm
  - Standard deviation of 1.74 times mean diameter

Aerodynamic drop fragmentation

Sandia National Laboratories

Motivation: fundamental spray process and an important canonical problem for multiphase simulations

- No viable methods to measure secondary drop size/velocity statistics or the 3D morphology of the ring shaped ligament

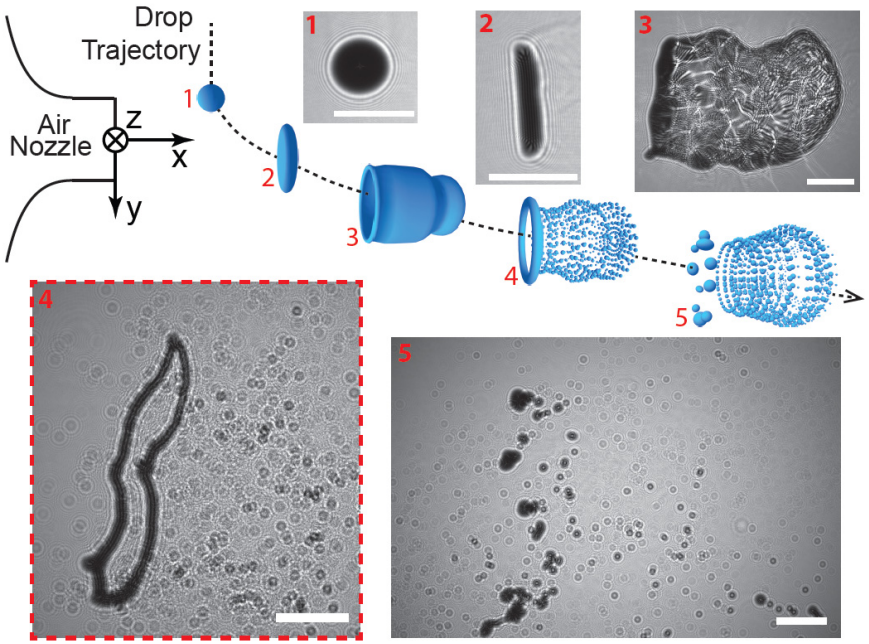

digital holograms of the breakup of an ethanol drop in an air-stream (Gao et al 2013, *Opt. Lett.*)

Experimental configuration: Double-pulsed laser and imaging hardware as typically used in PIV

- λ = 532 nm, 5 ns pulsewidth
- Interline transfer CCD (4008 × 2672, 9 μm pixel pitch)
- Temporal separation, Δt = 62 μs, determined by laser timing
  - Note: experiments in Guildenbecher et al, 2013, *Proceedings of Digital Holography and 3-D Imaging* confirm no loss of accuracy due to the reduced coherence length of these lasers

Aerodynamic drop fragmentation

- Secondary drop sizes/positions extracted by the hybrid method
  - Comparison with phase Doppler anemometer (PDA) data confirms accuracy of measured sizes

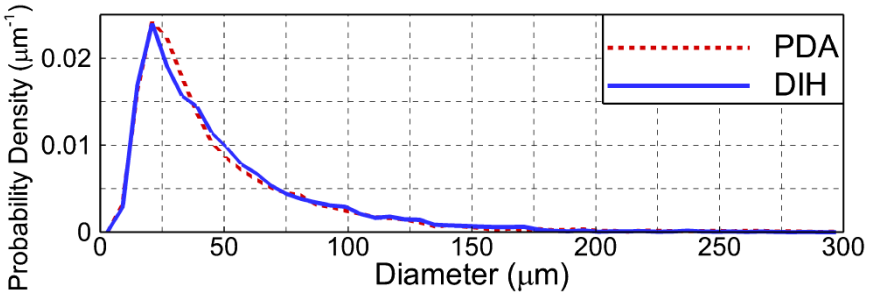

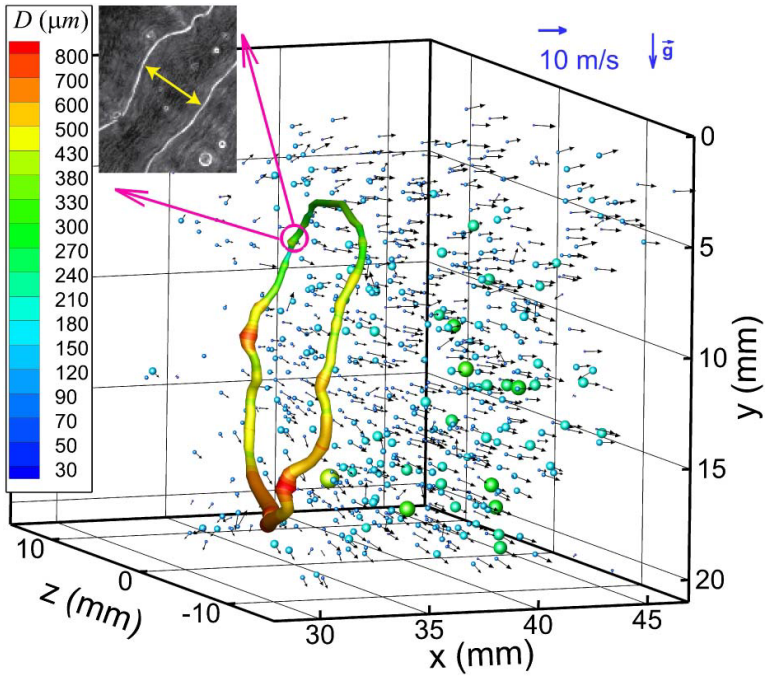

- Ring measured from *z*-location of maximum edge sharpness
  - Total volume of ring + secondary drops is within 2.2% of the initial volume
- 3C velocity measured by particle matching between successive frames
  - Expected symmetry observed with higher uncertainty in *z*-direction

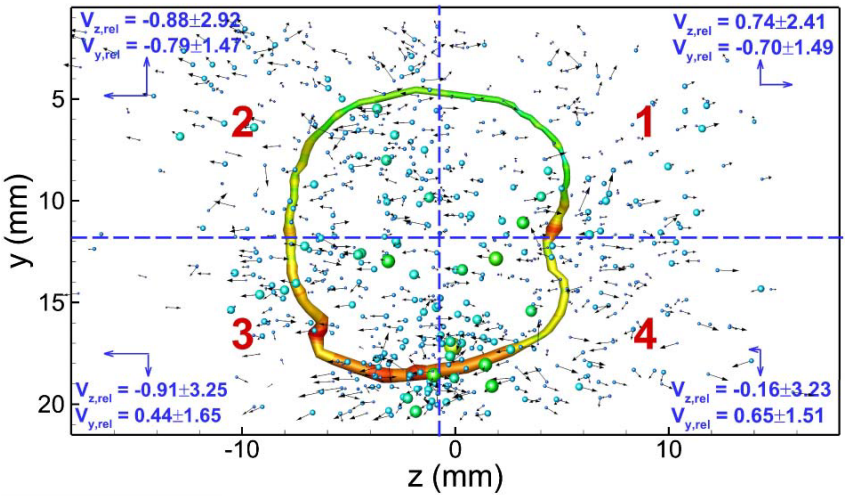

Aluminum drop combustion in propellants

Sandia National Laboratories

Motivation: Aluminum is added to solid propellant to increase specific impulse and reduce combustion instabilities

- At the burning surface, aluminum agglomerates to produce molten drops with a broad size distribution
- Predictive models require high-fidelity measurements

http://spaceflight.nasa.gov/gallery/images/shuttle/sts-120/html/sts120-s-028.html

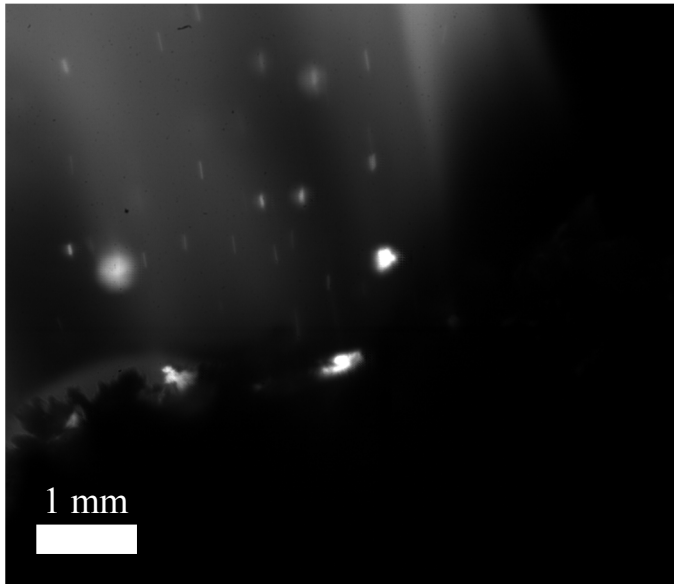

high-speed video of burning propellant strand

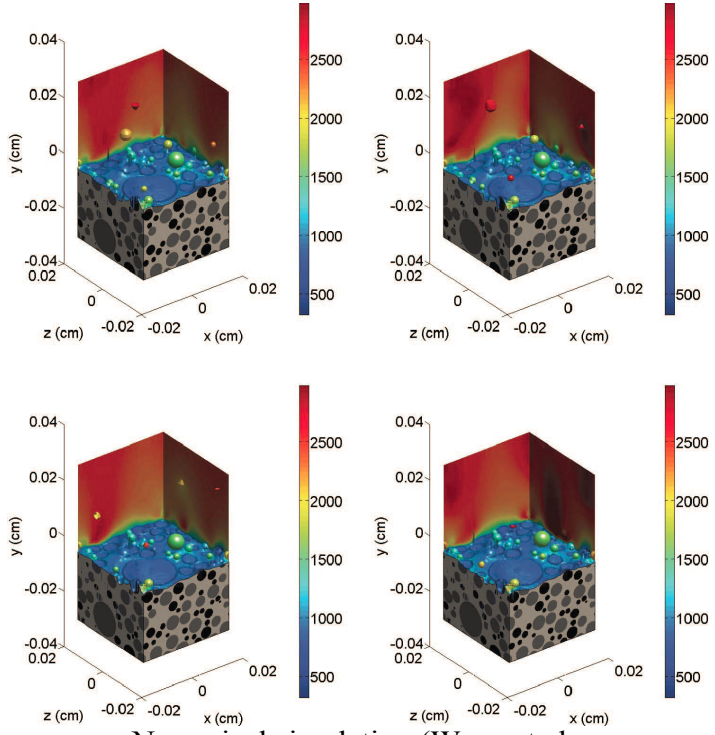

Numerical simulation (Wang et al., 2007, *Combust. Theor. Model.*)

Aluminum drop combustion in propellants

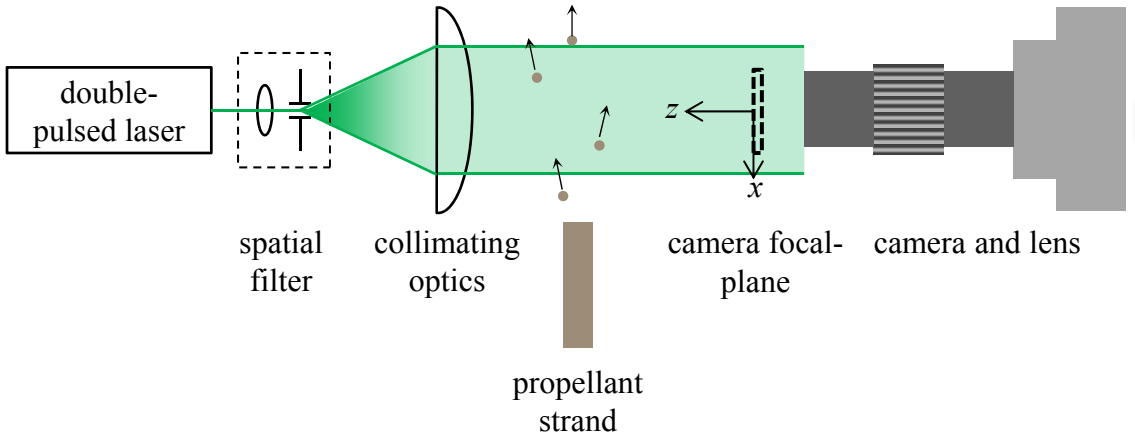

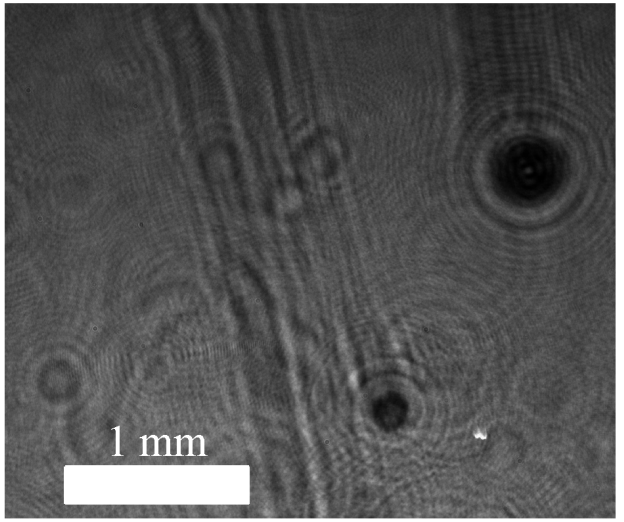

recorded hologram

Propellant: solid-rocket propellant pressed into a strand roughly 6 mm in diameter and initially 100 mm long

- Nominally 70 wt% ammonium perchlorate, 20 wt% aluminum particulate, 10 wt% hydroxyl terminated polybutadiene
- Combusts from the top surface down, ejecting molten aluminum particles traveling on the order of 10 m/s

Laser: Continuum Minilite Nd:YAG, 532 nm wavelength, 5 ns pulse duration

Camera: sCMOS from LaVision

Lens: Infinity K2 long distance microscope with CF-4 objective

Aluminum drop combustion in propellants

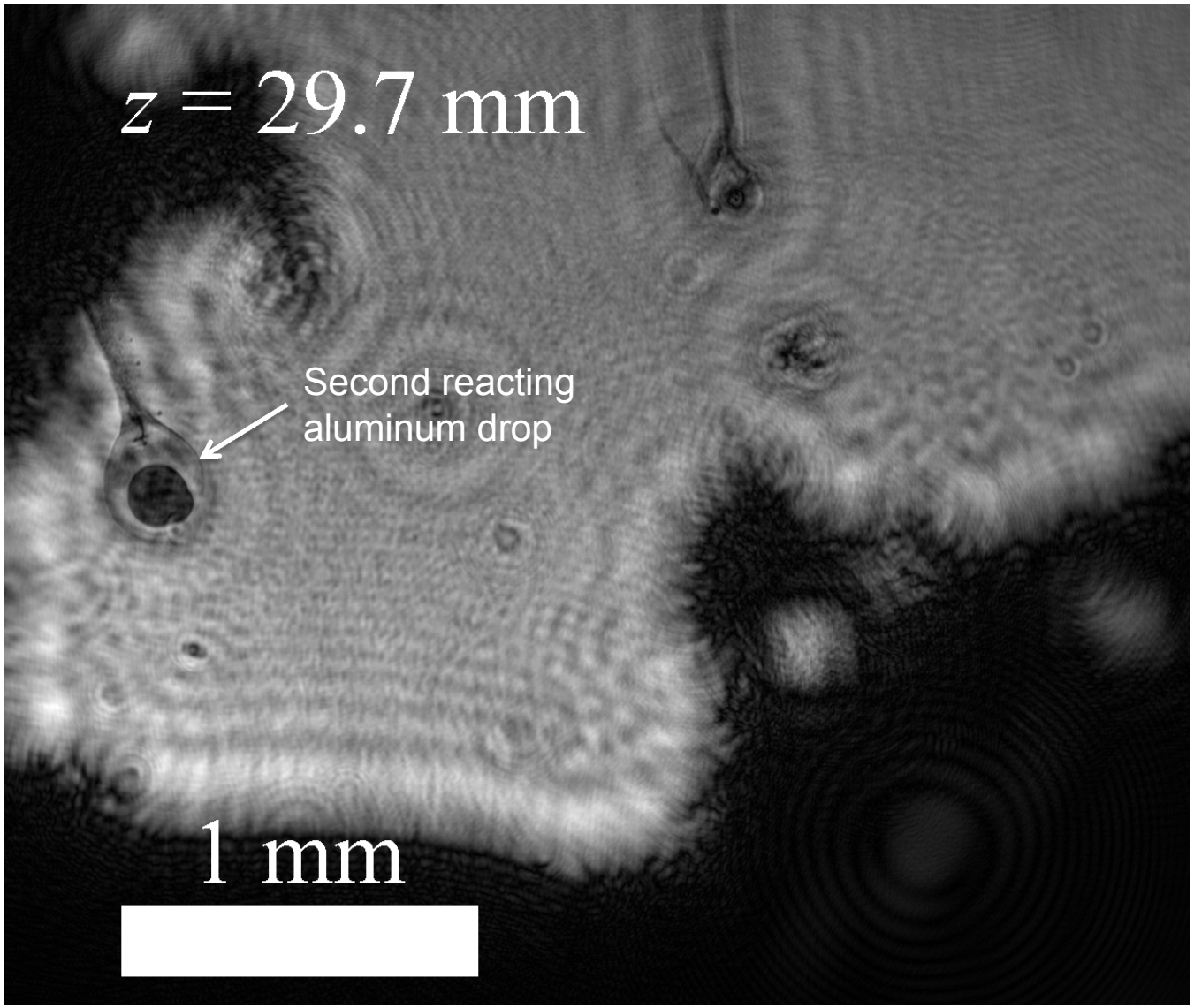

Aluminum drop combustion in propellants

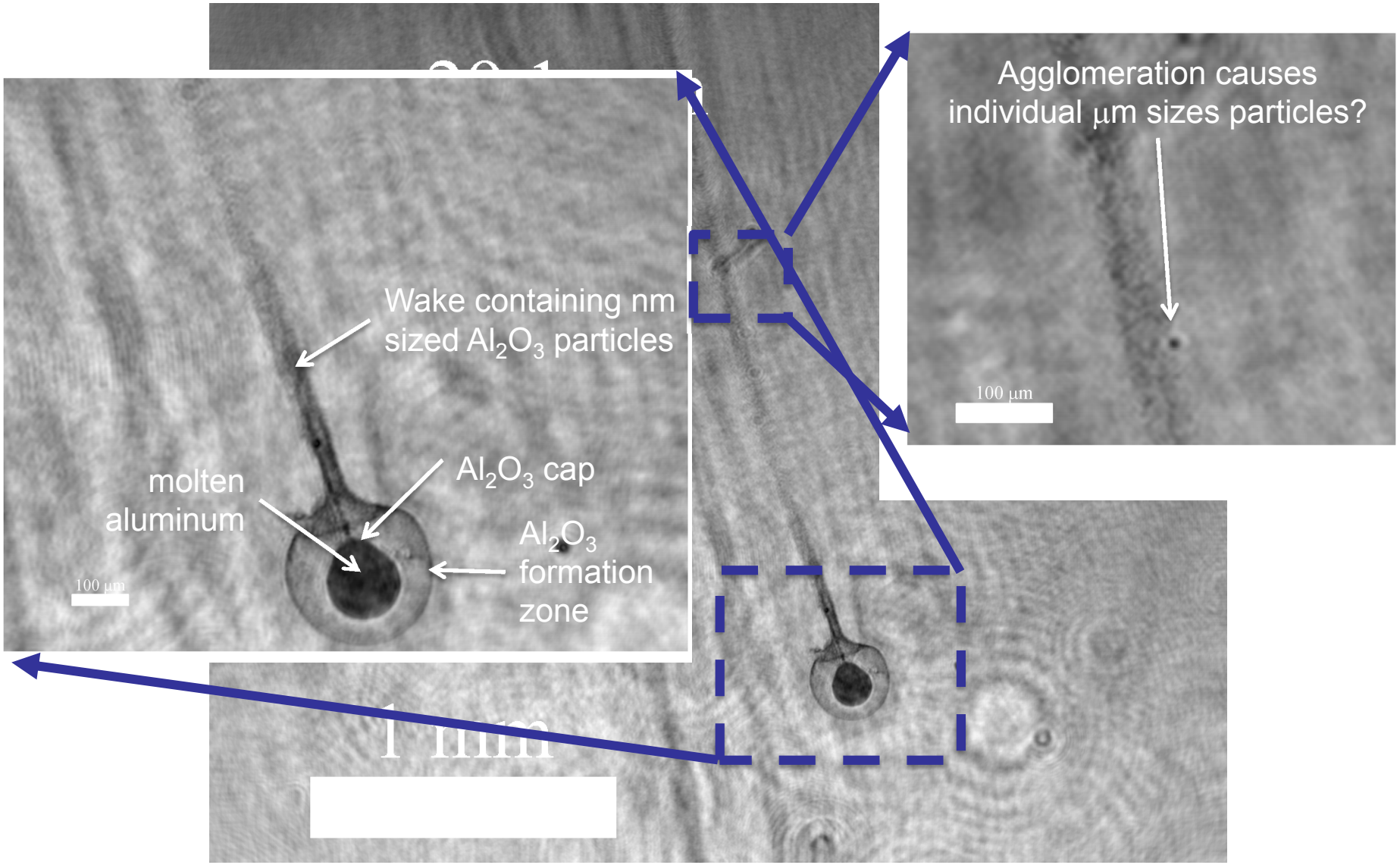

Aluminum drop combustion in propellants

Sandia National Laboratories

Digital holography allows for automatic measurement of in-focus features

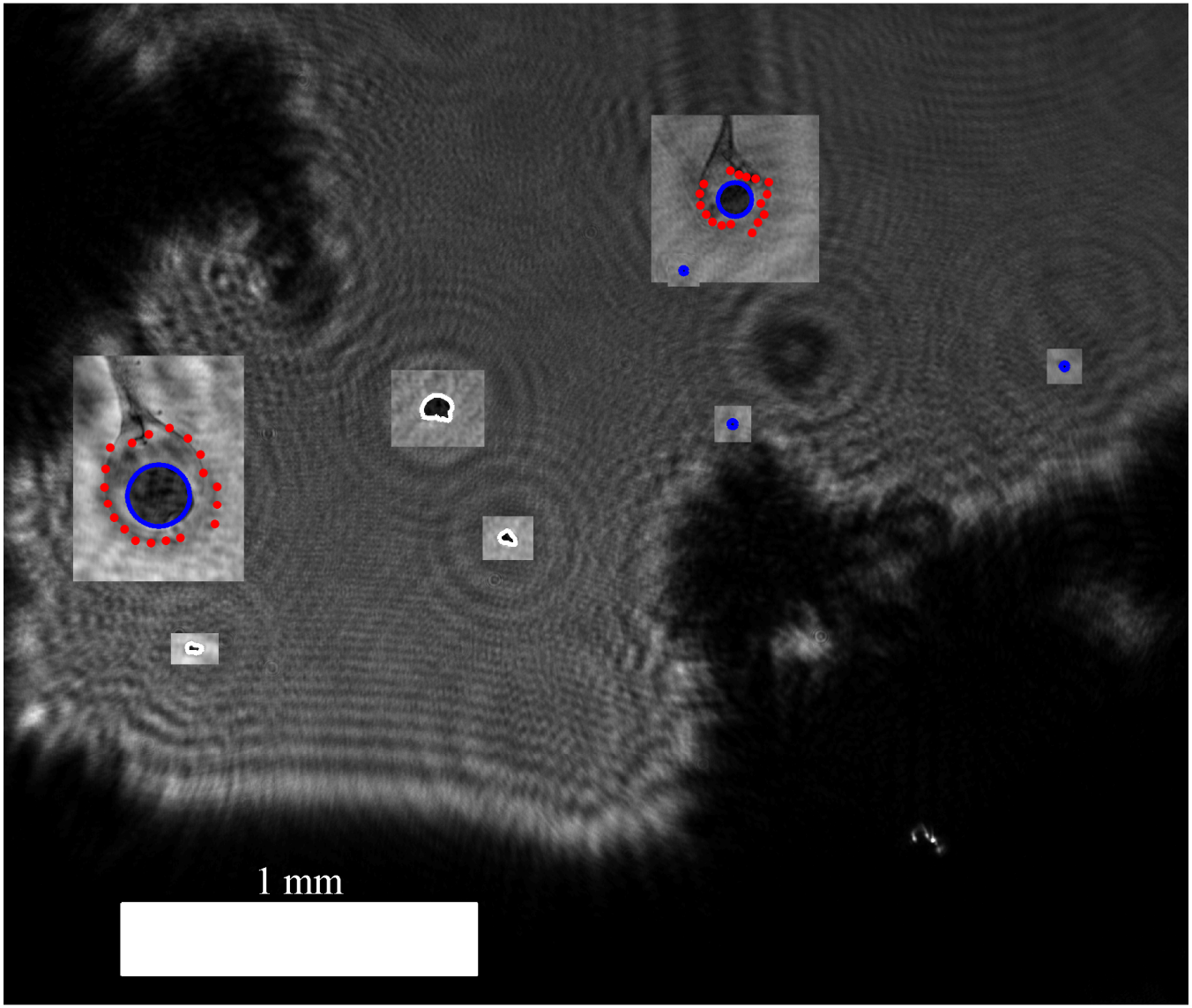

Aluminum drop combustion in propellants

Two strand burns → ~3000 images and 12000 measured drops

- Main peak due to agglomerated particulates
- Peak at 50 μm due to non-agglomerated particulate

Experiments repeated at higher initial temperature (faster burn rate)

- Main peak is reduced due to decreased residence time for agglomeration
- Peak at 50 μm remains

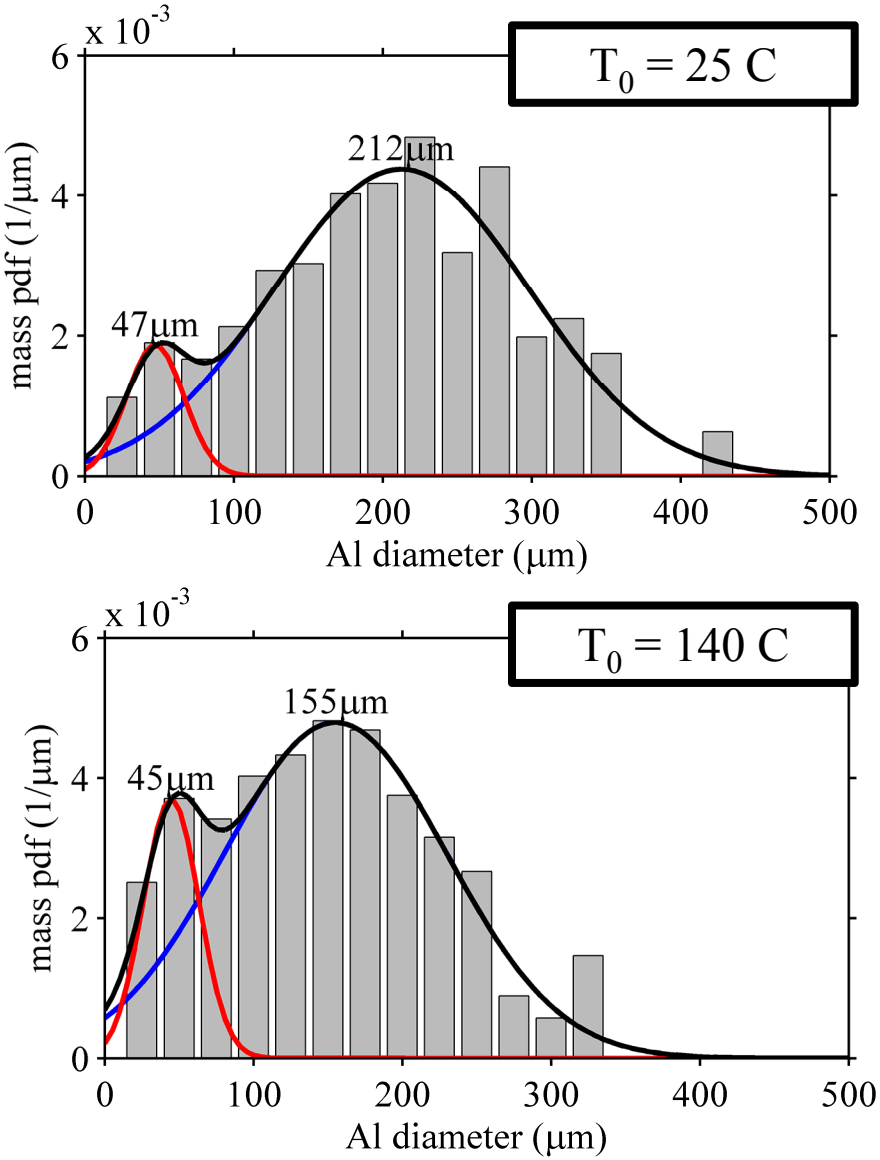

* Many thanks to Marcia Cooper, Mike Oliver, and Lee Stauffacher during these challenging experiments

Conclusions

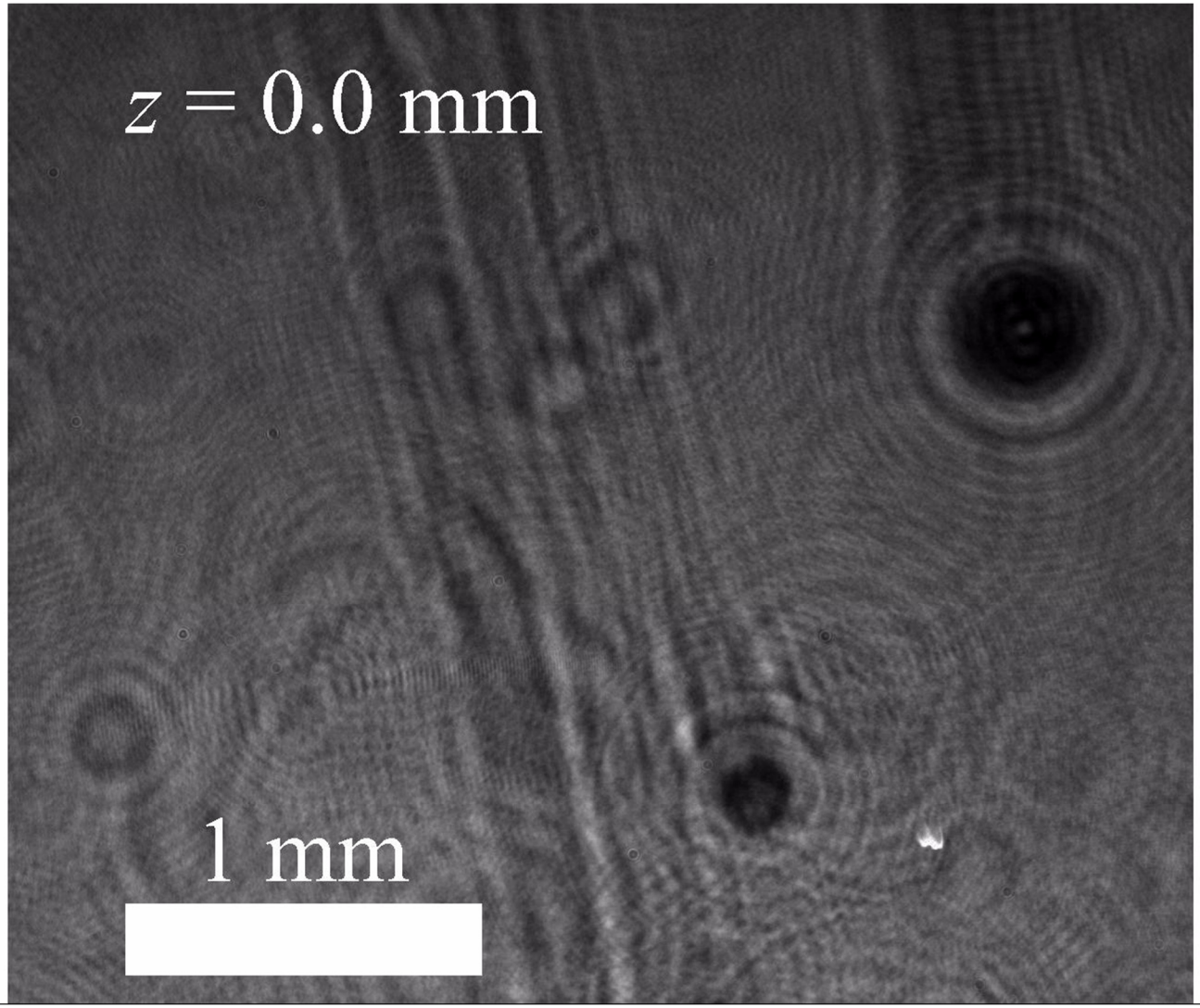

Developments in DIH enable quantitative 3D measurement of challenging multiphase flows with validated accuracy

Acknowledgements

- This work was supported by the California Institute for Technology—Jet Propulsion Laboratory Work for Others Contract 15110718.
- Additional support from the Weapons Systems Engineering Assessment Technology program and the Laboratory Directed Research and Development program at Sandia National Laboratories
- Significant collaborators include Marcia Cooper, Phillip L. Reu, Jian Gao, Jun Chen, Thomas Grasser, Daniel Scoglietti, Lee Stauffacher, Mike Oliver, Luke Engvall, Walt Gill, and many others….

Backup slides

Aluminum drop combustion in propellants

Sandia National Laboratories

<u>Open questions affecting image quality:</u>

1. What is the role of gas-phase thermal gradients?
   - Expected to lead to index of refraction variations
   - Numerical refocusing equations implicitly assume constant index of refraction

2. How do sub-μm alumina particles affect image formation?
   - Multiple scattering would lead to loss of phase information

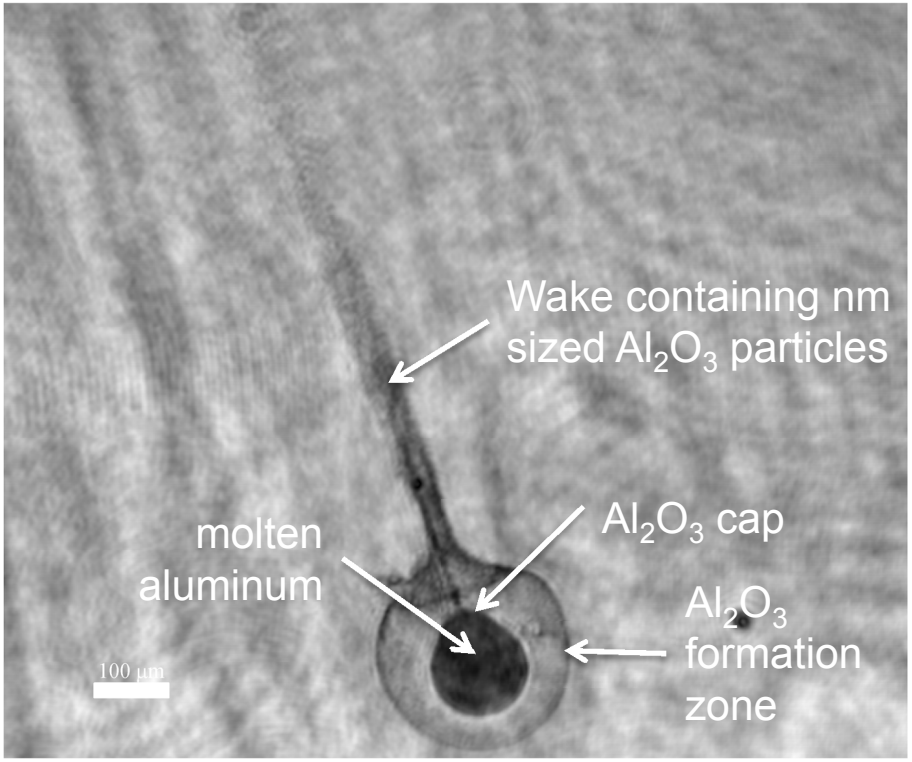

Experimental configuration for *z* validation

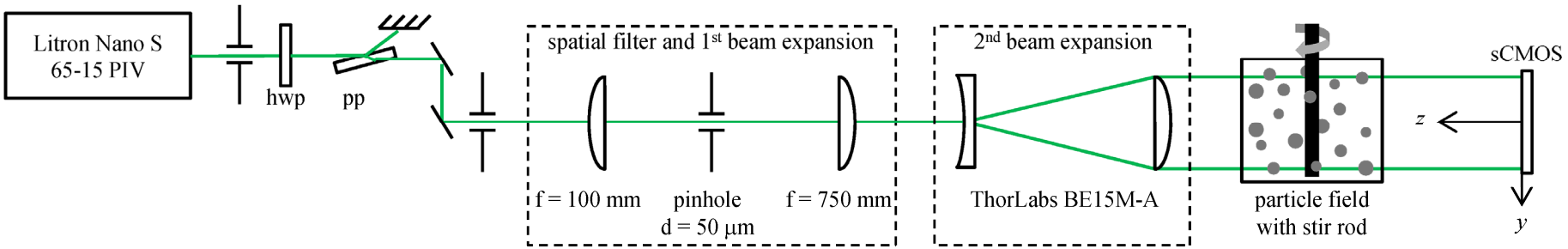

- Particles stirred by a rotating rod (r_0 = 1.58 mm, ω_0=100 rpm)
- Recorded at 15Hz with a LaVision sCMOS camera (2560 × 2160, 6.5 μm pixel pitch)

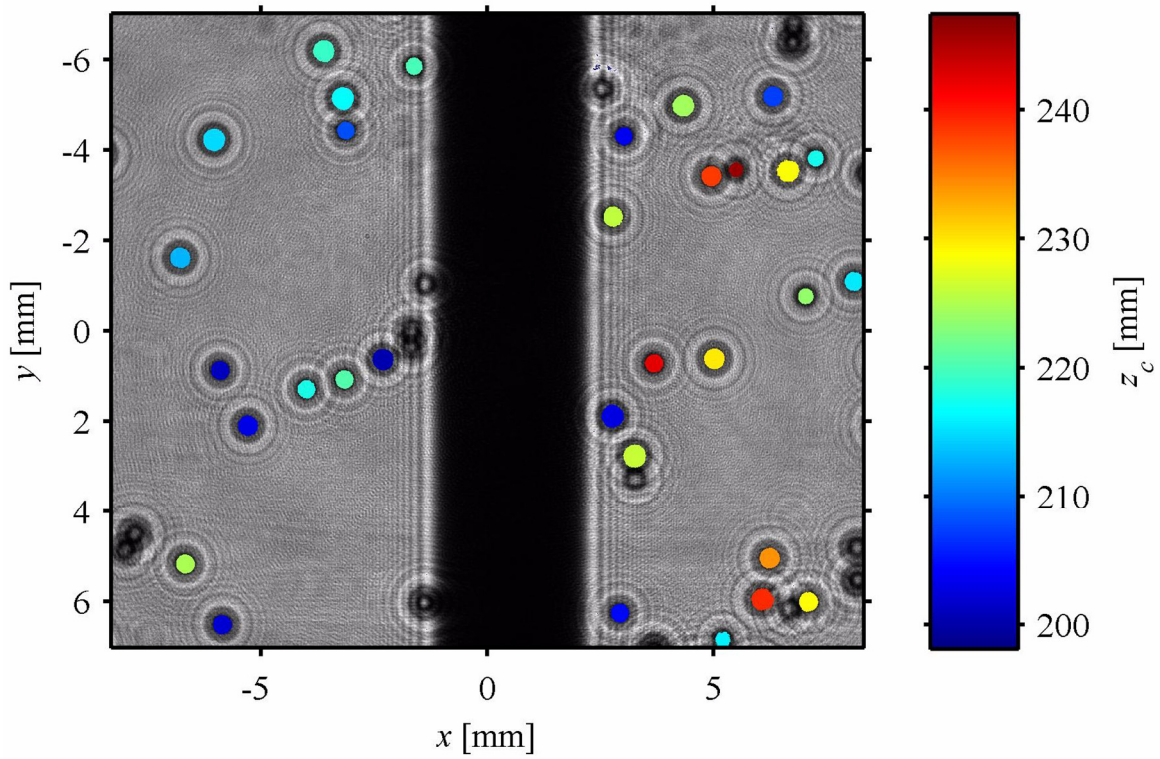

particles measured with the hybrid method, background shows the recorded holograms

Extraction of theoretical trajectory

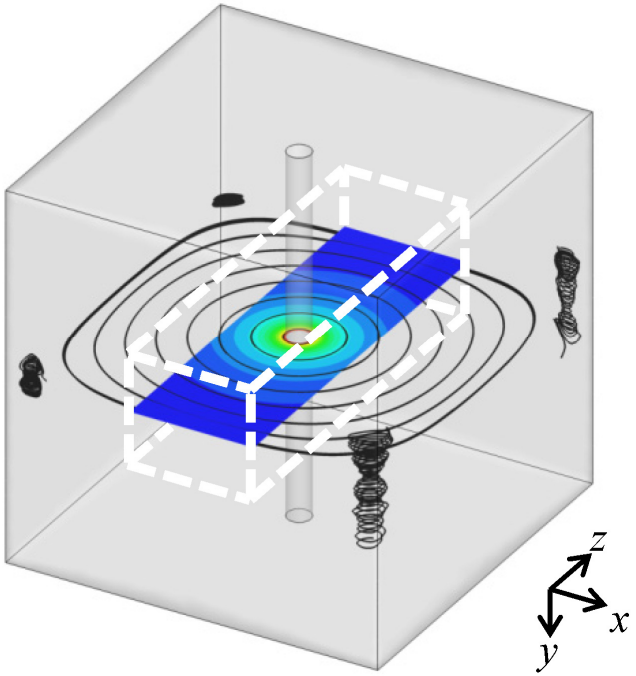

simulated flow field showing streamlines and total velocity contour within the center *x*-*z* plane of the field of view (dotted lines)

In the *x*-*z* plane, particles are expected to travel in near perfect circles

$$x(t) = r\cos(\omega t + \theta_0)$$

- Assuming measured *x*-positions have minimal error, curve fit → r, ω, θ_0

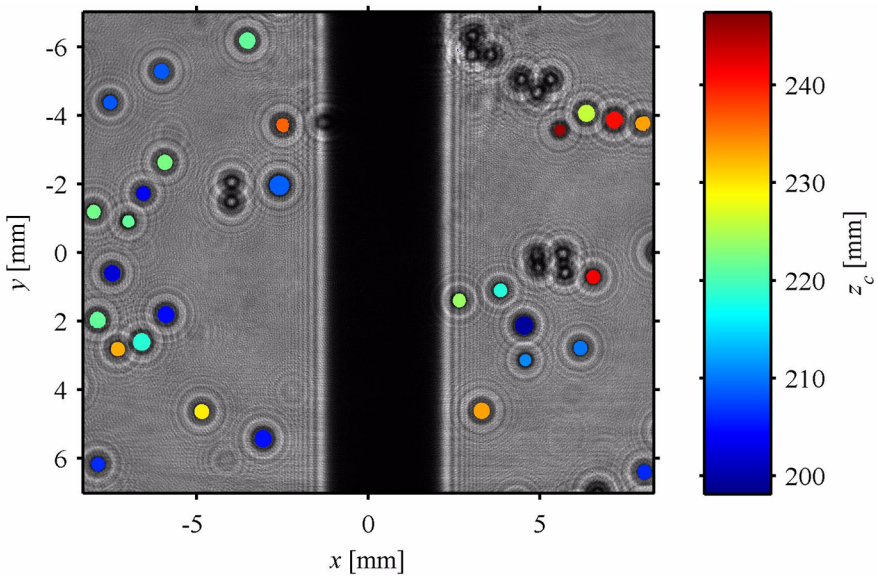

example in-plane trajectory

- Measured r = 5.04 mm, ω = 9.414 rpm
- At this r, simulation gives ω = 9.406 rpm

Comparison with measured results

Predicted *z*-trajectory: $z(t) = r\sin(\omega t + \theta_0)$ and $\Delta z(t) = r\omega\cos(\omega t + \theta_0)\cdot\Delta t$

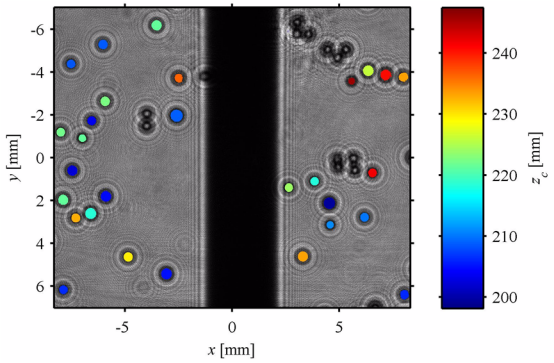

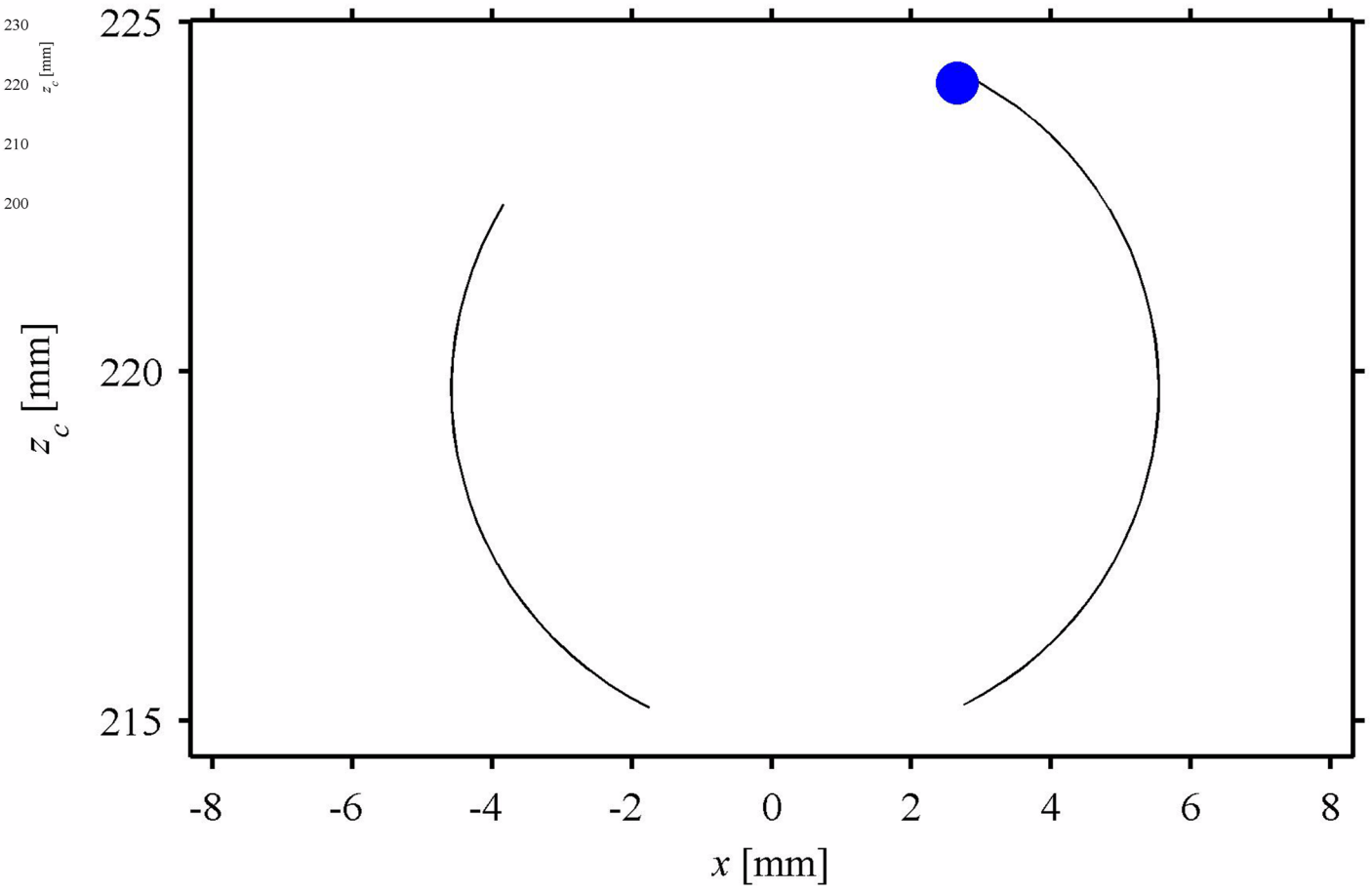

measured x-z trajectory vs. predicted

Conclusions

For all trajectories

- Error in measured z = -0.04 ± 1.51 mm
- Error in measured Δz = -0.03 ± 1.05 mm
  - Standard deviation of $2.3 \cdot \bar{d}$

Experiments repeated with smaller particles ($\bar{d} = 118 \mu m$, see paper for details)

- Error in measured z = -0.003 ± 0.379 mm
- Error in measured Δz = -0.001 ± 0.302 mm
  - Standard deviation of $2.6 \cdot \bar{d}$

Next steps:

- Compare results with alternative particle detection methods
- Use results to quantify effects of particle overlap and other experimental noise sources

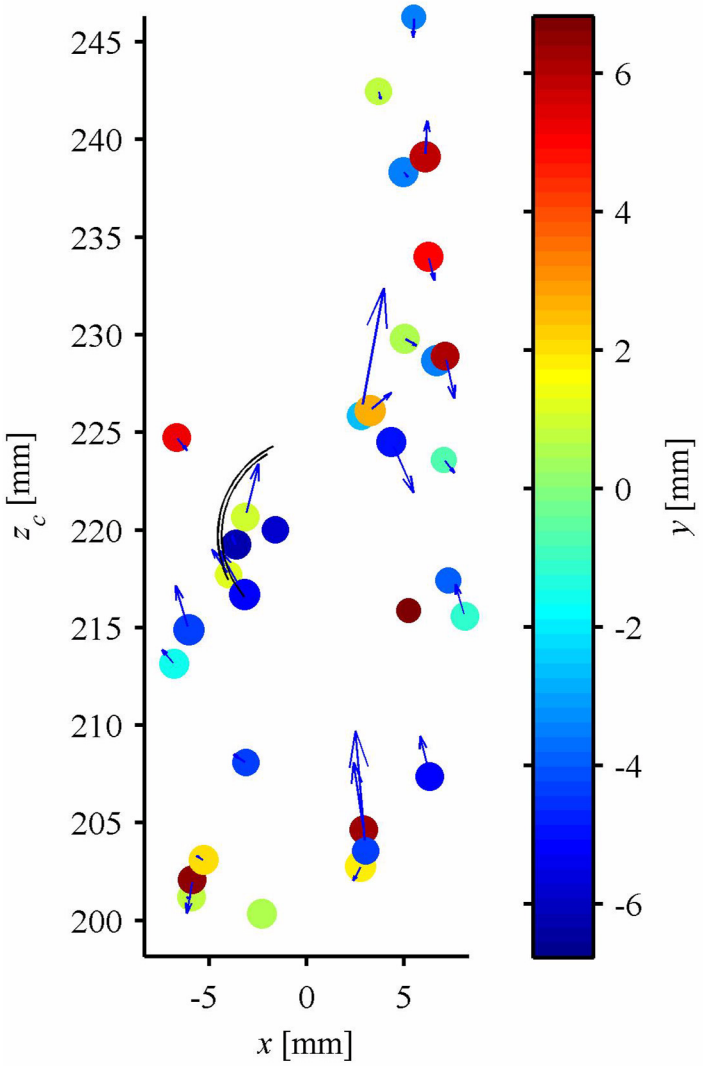

all measured x-z trajectories vs. predicted

3D, 3C fluid velocity measurements?

Advantages:

- Simple optical setup requiring only one line-of-sight view
- Large depth of field (hundreds of mm possible)
- Particle sizes can be measured (if desired)

Challenges:

- High uncertainty in the *z*-direction
- Particle field must be relatively sparse providing only limited vectors
- Vectors at random positions
- Methods not as mature as PIV or even tomographic-PIV

Note: the literature contains many works on holographic-PIV. My own work has not been focused on these applications

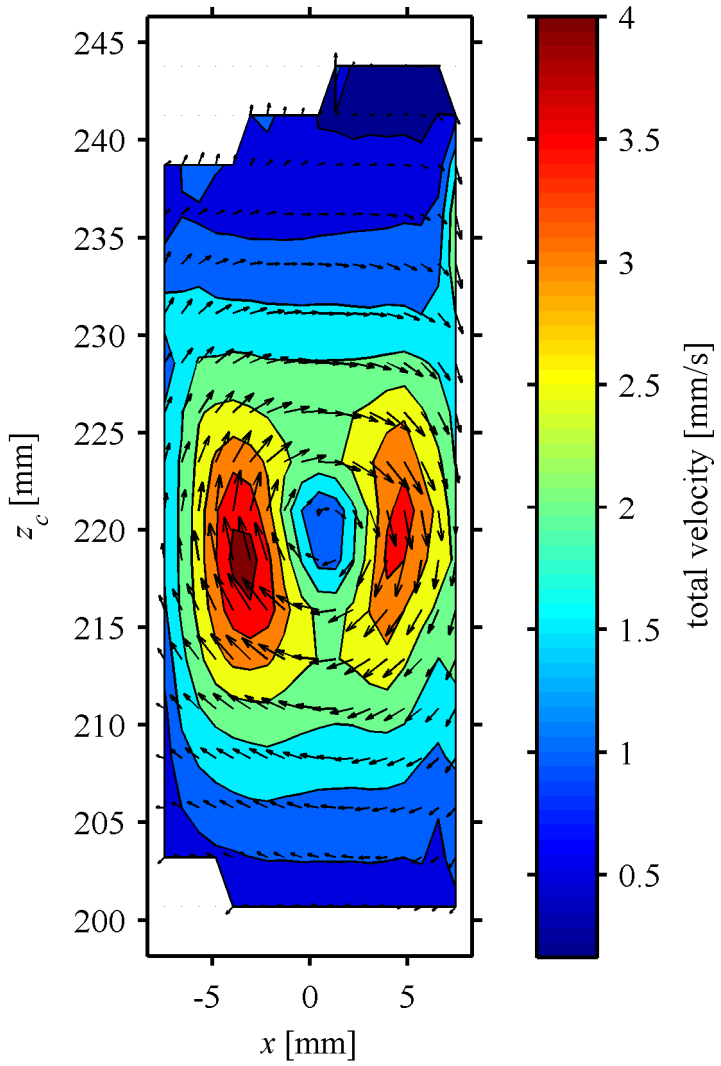

mean measured *x*-*z* velocities